

Article

A Study of Hygroscopicity Improvements to Adsorbents in Solar-Powered Air Water Extraction

Yao Lv, Jiangbo Wu ^{*}, Jiewen Dong and Tingwei Jia

School of Energy and Power Engineering, Lanzhou University of Technology, Lanzhou 730050, China; djiewen@icloud.com (J.D.); superbjtw@outlook.com (T.J.)

* Correspondence: wujb@lut.edu.cn

Abstract: As a global freshwater shortage is imminent, solar-powered adsorption-based atmospheric water harvesting technology is gradually attracting people's attention due to its environmental friendliness and many other advantages. Among the many adsorbents used in this technology, MOF-801 has a large adsorption capacity in a wide range of humidity. In the current field, carbon materials are usually added to improve the photothermal properties of MOF-801, but hybrid adsorbents made in this way usually weaken the adsorption performance of MOF-801. If the MOF-801/carbon material adsorbent is used as a base and mixed with hygroscopic salt, which also has good adsorption properties, the hygroscopic properties of MOF-801 can be improved and the drawback of hygroscopic salt, which is prone to be lost after absorbing water, can be ameliorated. In this study, a hybrid adsorbent combining MOF-801 with carbon black (CB) and LiCl was prepared, and the effects of carbon black and LiCl on the performance of the MOF-801 adsorbent were compared. The experiments showed that the adsorption capacity of the hybrid adsorbent obtained a significant enhancement after the addition of LiCl, which increased by 38.2% versus 112.3% compared with MOF-801 and MOF-801/CB.

Keywords: atmospheric water harvesting; solar water harvesting; MOF-801 adsorbent; hygroscopic salt



Citation: Lv, Y.; Wu, J.; Dong, J.; Jia, T.

A Study of Hygroscopicity Improvements to Adsorbents in Solar-Powered Air Water Extraction. *Coatings* **2024**, *14*, 472. <https://doi.org/10.3390/coatings14040472>

Academic Editor: Hyung-Ho Park

Received: 8 March 2024

Revised: 5 April 2024

Accepted: 11 April 2024

Published: 12 April 2024



Copyright: © 2024 by the authors. Licensee MDPI, Basel, Switzerland. This article is an open access article distributed under the terms and conditions of the Creative Commons Attribution (CC BY) license (<https://creativecommons.org/licenses/by/4.0/>).

1. Introduction

With the growing population and the continuous economic and social development of mankind, many countries and regions of the world are currently facing a serious shortage of freshwater resources [1–3]. Against the backdrop of the global freshwater crisis, there is an urgent need for new technology that can feasibly solve this problem. The solar-powered adsorption method for air water extraction can utilize the abundant light resources in arid regions to obtain large amounts of freshwater resources in the atmosphere. The principle is to use an adsorbent to absorb water vapor in the air, desorb the water and collect it under solar heating, and recycle the desorbed adsorbent again [4,5]. The moisture in the atmosphere is naturally replenished by the water cycle, so there is no disruption to the water vapor cycle or the natural environment. The water collected in the device is very clean and hygienic, and after simple treatment, it can be used for daily household or agricultural production. At the same time, compared with other air water extraction methods, the solar adsorption air water extraction method is not subject to power constraints and is suitable for a variety of extreme climates, has greater potential for application in a wide range of application scenarios, and has received a lot of attention from scholars.

The process of solar adsorption air water extraction systems is mainly divided into two phases of adsorption and desorption, which gave birth to the most basic system design in use today, taking into account night temperature differences in the desorption and adsorption of intermittent water extraction systems [6–8]. In contrast, continuous airborne water extraction systems perform the adsorption and desorption processes several times a day, and are an improvement upon and development of the intermittent system.

Continuous systems can increase daily water production by allowing multiple cycles in a day. However, more stringent requirements are placed on the adsorbent, which not only needs to have a high adsorption capacity, but also needs to have both fast adsorption and desorption capacities and cycle stability. Therefore, the ideal adsorbent should have the characteristics of high moisture absorption, a fast moisture absorption speed, a wide working field (moisture absorption in a wide range of humidity can be increased with the increase in humidity), the ability to be driven by solar energy and other relatively low-temperature heat sources, efficient and rapid desorption, and a long cycle life.

Among many adsorbents, hygroscopic salts [7,9–11] have better water extraction performance; the ions in its crystal structure will interact with water molecules to form hydrogen bonding, thus adsorbing water molecules on the surface or internal structure. Kabeel et al. [12] used CaCl_2 as an adsorbent for water extraction experiments, and their device could obtain a water production rate of up to $2.5 \text{ L}/(\text{day}\cdot\text{m}^2)$ under ideal conditions. However, since it will dissolve in the water produced, the performance is difficult to regulate, is prone to system corrosion, etc. Srivastava et al. [13] proposed a method of encapsulating hygroscopic salt into other matrices by mixing LiCl with silica, which greatly limited the adverse effects caused by the dissolution of the salt in the device after the absorption of water, and obtained $115 \text{ mL}/\text{day}$ at $\text{RH} = 20\%$ of the water withdrawal rate.

Meanwhile a novel material, MOFs (metal–organic frameworks), shows potential as an air water extraction adsorbent, with a pore structure and chemistry that can be tuned at the molecular level by different ligands [14–17]. This type of adsorbent has a large number of complex cavities, which allows it to maintain a high rate and amount of moisture absorption in low-temperature and arid environments. Yaghi et al. [16,18] in *Science* reported that the MOF-801 adsorbent possesses excellent adsorption characteristics, with the advantages of a fast desorption time and high cyclic stability. However, the desorption temperature of pure MOF-801 is extremely high and its solar energy utilization efficiency is low. In order for this adsorbent to be driven by solar energy and other low-temperature heat sources for air water extraction, scholars mixed MOF-801 with a variety of carbon-based materials to improve its photo-thermal properties, along with slightly reducing the saturated adsorption capacity, and they increased the adsorption and desorption efficiency and improved the amount of water produced. On this basis, if this MOF-801 hybrid adsorbent is used as a substrate and combined with hygroscopic salt, it is expected to develop a new type of composite adsorbent with a higher rate and amount of moisture absorption.

In this study, a composite adsorbent based on MOF-801, carbon black (CB), and LiCl was prepared with the objective of applying it in a continuous solar adsorption air water extraction system, and adsorbent performance testing experiments were established. The experiments verified that the adsorbent has excellent hygroscopic properties, and the hygroscopic performance is greatly improved compared with that of the MOF-801 adsorbent. The results showed that this adsorbent has great potential for application in solar air water extraction devices.

2. New Composite Adsorbent Preparation and Experimental Device Production

Composite adsorbents, which are novel adsorbents consisting of one or more materials, such as matrix plus hygroscopic salts [13,19,20], carbon materials, porous media [21,22], etc., have shown great potential in the last 20 years of development.

In the preparation of the hybrid adsorbent, MOF-801 and carbon black (CB) powder were firstly mixed thoroughly in a certain ratio to make an MOF-801/CB adsorbent in the form of black powder. Subsequently, the powder was immersed in LiCl solution, the MOF-801/CB and LiCl were mixed homogeneously by stirring and standing, and the MOF-801/CB-LiCl adsorbent was made after drying.

In these materials, CB is added to improve the photothermal properties of the materials so that they show better performance in the resolution process. Meanwhile, the MOF material was combined with LiCl to provide a good attachment environment for the salt

with strong hygroscopicity, and at the same time, the hygroscopicity of the composite adsorbent and the stability of the salt were improved.

2.1. Parameters of the MOF-801/CB Substrate

For the fabrication of MOF-801/CB, 67:33 wt% was chosen as the specific gravity of the two components, a ratio that has been proven to be feasible in the Yaghi team study [16,18]. Depending on the laboratory conditions, wet ball milling was carried out using a ball-milling machine (QM-3SP04, NJU-instrument, Nanjing, China) to make a more homogeneous mixture of the two materials. CB and MOF-801 were ground and mixed in an agate ball-milling jar at a ratio of 67:33 wt%, and the grinding beads were zirconia beads with methanol as the dispersion. Subsequently, the mixed suspension was placed in a vacuum freeze-dryer (LYO QUEST-55, Telstar, Barcelona, Spain) and dried in a $-40\text{ }^{\circ}\text{C}$ environment for a period of 3 days to produce the substrate of the composite adsorbent. The appearance of the two powders, MOF-801 and MOF-801/CB, is demonstrated in Figure 1.



Figure 1. Form of MOF-801 and MOF-801/CB.

Both adsorbents were tested using the BET specific surface area and pore analysis (By a Micromeritics ASAP 2460, Micromeritics Instrument, Norcross, GA, USA) to analyze the effect of the added CB on the pore structure of MOF-801. From the test results, it was found that the BET specific surface area of MOF-801 was $511.49 \pm 3.95\text{ m}^2/\text{g}$, while that of MOF-801/CB was $486.45 \pm 7.59\text{ m}^2/\text{g}$. The adsorption average pore size of MOF-801 was $3.38 \pm 0.009\text{ nm}$, while that of MOF-801/CB was $4.26 \pm 0.013\text{ nm}$. It can be seen that the black CB improved the MOF-801's photothermal properties, while the larger particle size of CB also better maintains the adsorption structure of the hybrid material, providing favorable conditions for the attachment of hygroscopic and hygroscopic salts. Figure 2 demonstrates the nitrogen adsorption/desorption curves of the two adsorbents at 77 K.

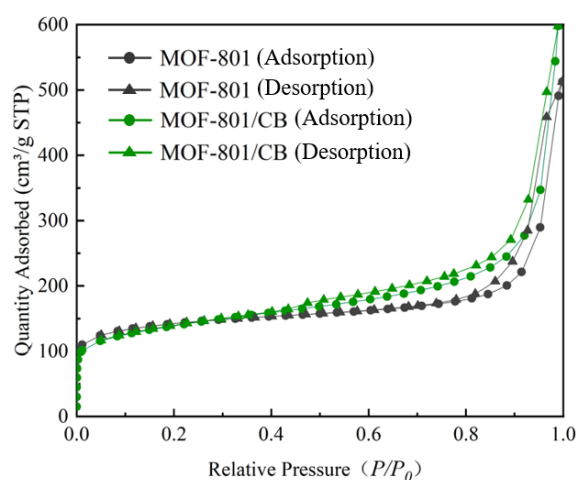


Figure 2. The N_2 sorption isotherms at 77 K of MOF-801 and MOF-801/CB.

As can be seen in Figure 2, the adsorption of N_2 in the low-pressure region of the relative pressure P/P_0 ($P/P_0 \leq 0.1$) increases rapidly with the increase in the relative pressure, and the growth of the adsorption of N_2 slows down after $P/P_0 > 0.1$. The hysteresis loop for the adsorption of MOF-801/CB occurs at the position of $P/P_0 \geq 0.4$, and the hysteresis loop for the adsorption of MOF-801 occurs at the position of $P/P_0 \geq 0.8$. The results of the curves showed that both adsorbents possessed a large number of micropores and the distribution of the pore sizes was also wide, with a small number of mesopores present. And MOF-801/CB has higher porosity and a greater N_2 adsorption capacity.

2.2. Preparation of MOF-801/CB-LiCl Adsorbent

After the MOF-801/CB was fabricated, it was fully mixed with LiCl by means of salt solution immersion. In order to avoid the influence of impurities such as alcohol in the adsorbent substrate on the experimental results, it was necessary to activate the MOF-801/CB before combining it with LiCl. An appropriate amount of MOF-801/CB was weighed and placed in a glass Petri dish, which was then put into a vacuum-drying oven at high temperature for 12 h. The temperature was set at 120 °C and the vacuum degree was set at 133 Pa to obtain sufficiently dried MOF-801/CB. Subsequently, different mass fractions of LiCl solutions were configured and prepared for mixing the two materials.

In the subsequent adsorption experiments, we found that the specific gravity of LiCl should not be too high when mixing the adsorbent. Although more salt will significantly enhance the moisture absorption of the composite adsorbent, such an adsorbent in the saturated state will not be able to maintain a more compact solid state due to the absorption of too much water, and even has a certain degree of mobility, which is not conducive to the design and maintenance of the air water extraction device. Therefore, we chose the mixing ratio of 1 g of MOF-801/CB mixed with 5 mL of LiCl solution with a mass fraction of 10%.

Subsequently, the mixed suspension was placed in a beaker and fully mixed by a magnetic rotor mixer (MS7-H550-Pro, DLAB, Beijing, China) at a speed of 1000 r/min and a mixing time of 2 h. The well-mixed suspension was allowed to stand at room temperature for 24 h to allow the materials to be well-mixed. Subsequently, the MOF-801/CB-LiCl suspension was placed in a Petri dish and dried at high temperature in a vacuum-drying oven for 24 h. The temperature was set to 80 °C and the vacuum was set to 133 Pa. As the drying time increased, the mass of the mixed adsorbent did not change any more, and the fully dried MOF-801/CB-LiCl adsorbent was obtained.

2.3. Structural and Elemental Analysis of Composite Adsorbents

In order to confirm the composition of the MOF-801/CB-LiCl composite adsorbent, as well as the interaction between the three materials, the microstructure and morphology of the composite adsorbent needed to be examined and characterized. The results of multiple analyses are shown in Figure 3.

As shown in Figure 3a, the indicated FTIR tests (By Nicolet iS20, Waltham, MA, USA) had a wave number range of 400 to 4000 cm^{-1} , and the number of scans was 32 with a resolution of 4 cm^{-1} . As shown in Figure 3, the FTIR spectra of the three adsorbents did not show significant differences in comparison with the peaks of MOF-801, which indicates that the functional groups of the composite adsorbents were basically the same as those of MOF-801.

The results of the XRD analysis (By Rigaku D MAX-2600, Tokyo, Japan) are shown in Figure 3b. $Cu K\alpha$ was selected as the radiation source to characterize the activated MOF-801 and MOF-801/CB powders by X-ray diffraction. The data were collected at an angle of 5–90 degrees, and the acquisition rate was 2 degrees/min. The diffraction peaks of the three composite adsorbents and MOF-801 were basically the same, and the crystal structure of MOF-801 did not show any major changes after mixing.

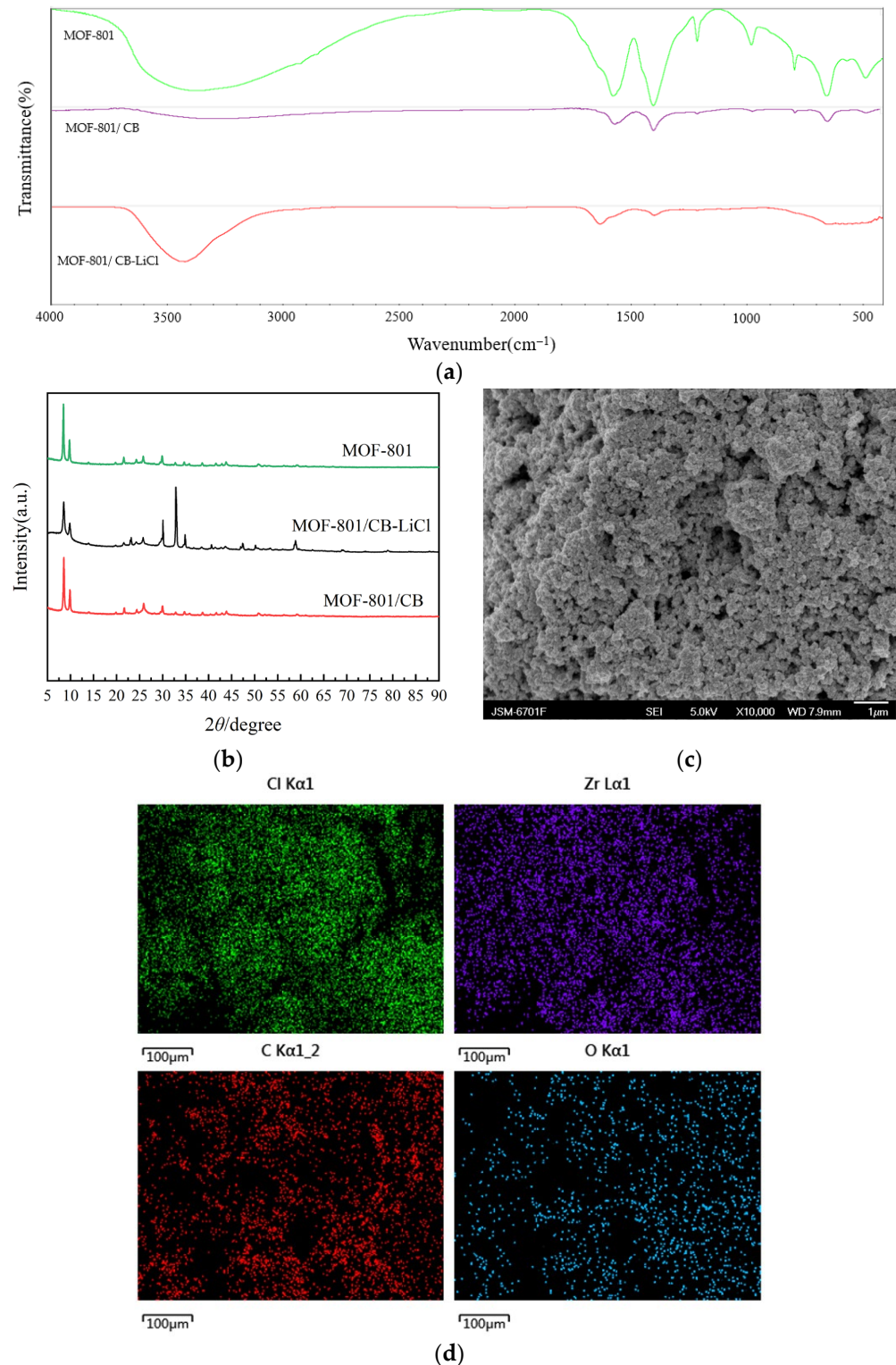


Figure 3. Structural and elemental analysis results of adsorbents: (a) FTIR images of three adsorbents; (b) XRD images of three adsorbents; (c) SEM image of MOF-801/CB-LiCl; (d) elemental distribution within MOF-801/CB-LiCl obtained by BDS analysis.

Figure 3c,d show the elemental distribution of MOF-801/CB-LiCl as demonstrated by the SEM image with BDS analysis (By JSM-5600LV, JEOL, Tokyo, Japan). In the figure, MOF-801, which has a granular microstructure, and other materials mixed with it can be seen, and there are a large number of pore structures inside the composite adsorbent, which facilitates the attachment of LiCl and the absorption of water. In the BDS analysis, the

distribution of various materials can be seen, and the results shown in the figure show that the mixing of various materials is relatively homogeneous.

3. Compound Adsorbent's Adsorption Characteristics: Testing Experiments

In order to investigate the effect of the addition of LiCl on the adsorption characteristics of the adsorbent, MOF-801, MOF-801/CB, and MOF-801/CB-LiCl adsorbents of the same mass were taken, and the adsorption rate and saturated adsorption amount of the three adsorbents were compared with each other in order to evaluate the effect of the new adsorbent by selecting a certain air temperature (T) and humidity (RH) as variables. According to the amount of adsorbent produced, a Petri dish with an inner diameter of 35 mm was selected as the container when conducting the experiment, and 200 mg of each adsorbent sample was evenly spread on the bottom of the dish. The Petri dish with the adsorbent was placed on an analytical balance, and then the balance was placed in a constant-temperature and -humidity chamber (Aikosp, Jiangsu, China) for adsorption. The change in the mass of the adsorbent within the analytical balance was recorded during the adsorption process, and when the mass of the adsorbent ceased to change, it indicated that the adsorbent had been absorbed to saturation.

3.1. Hygroscopic Properties of Composite Adsorbents

In order to compare the adsorption characteristics of the three adsorbents, three groups of samples were successively adsorbed to saturation at a temperature of $T = 25\text{ }^{\circ}\text{C}$ and a relative humidity of $\text{RH} = 20\%$, and the experimental results are shown in Figure 4. Among these three materials, MOF-801 was almost saturated after 9600 s, with a mass change of 22.8% and an adsorption amount of 0.228 Kg of water per kg of MOF, which is recorded as 0.219 kg/kg, similar properties to those of MOF-801 reported by Yaghi et al. [16,18]. MOF-801/CB was saturated at 7200 s, with a mass change of 14.9% and an adsorption amount of 0.149 kg/kg, while MOF-801/CB-LiCl was saturated after 10,800 s, with a mass change of 31.6% and an adsorption capacity of 0.316 kg/kg.

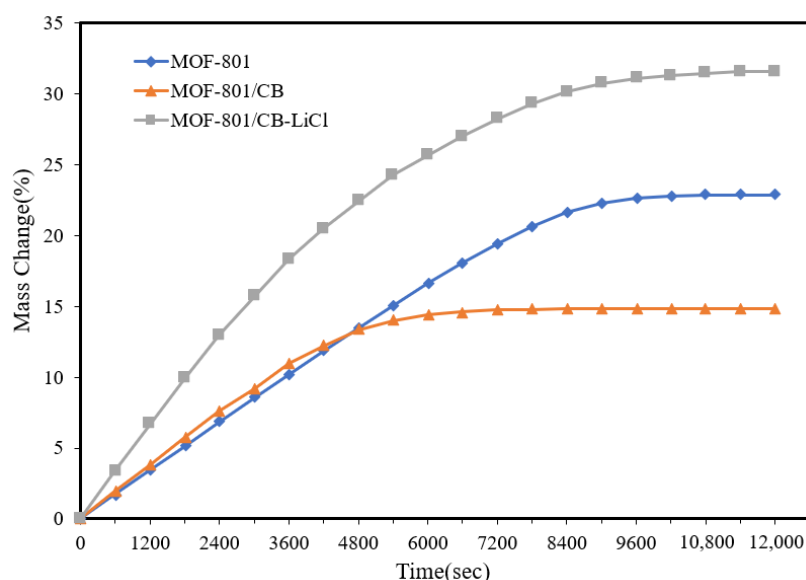


Figure 4. Comparison of adsorption characteristics of three adsorbents.

Each group of experiments was repeated three times and the average value was taken as the experimental result. Due to the difference in water absorption properties, after error analysis, the uncertainties of the three adsorbents, MOF801, MOF-801/CB, and MOF801/CB-LiCl, were 0.21%–0.41%, 2.17%–0.43%, and 0.71%–1.41%, respectively.

It can be seen that the addition of CB improved the adsorption rate of the adsorbent in the early stage of adsorption, but the effect on the microstructure of MOF-801 made the

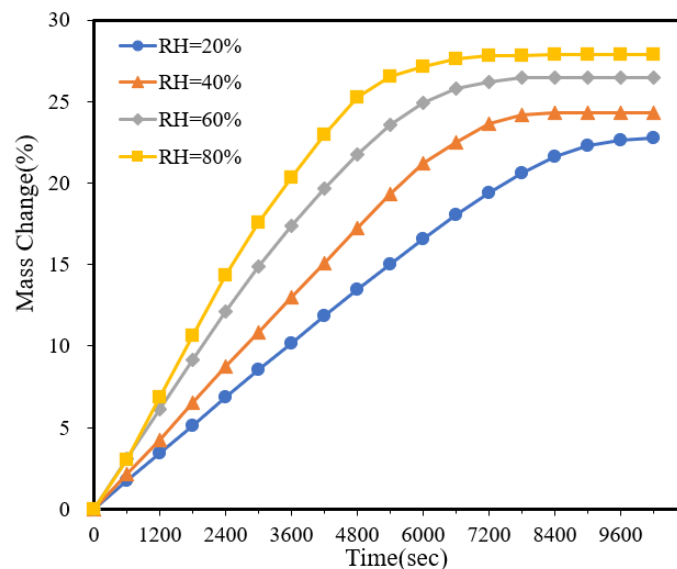
maximum moisture adsorption of the adsorbent decrease by 34.9%. After the addition of LiCl, which improves absorption characteristics, the adsorption capacity and adsorption rate of the adsorbent were greatly improved compared to the other two adsorbents, with an increase of 38.2% compared to MOF-801 and 112.3% compared to MOF-801/CB under the conditions of $T = 25\text{ }^{\circ}\text{C}$ and $\text{RH} = 20\%$.

3.2. Effect of Temperature and Humidity on the Adsorption Characteristics of Composite Adsorbents

The ability to adsorb over a wide range of humidity intervals is an important indicator for evaluating adsorbent performance. In order to investigate the effect of different humidity levels on the moisture adsorption characteristics of the composite adsorbent compared to the hybrid adsorbents, MOF-801, MOF-801/CB, and MOF-801/CB-LiCl were placed in a constant-temperature and -humidity chamber for adsorption experiments, with the settings of $T = 25\text{ }^{\circ}\text{C}$ and $\text{RH} = 20\%$, 40% , 60% , and 80% , and the change in the mass of the adsorbent was recorded until it reached saturation. The experimental results are shown in Figure 5.

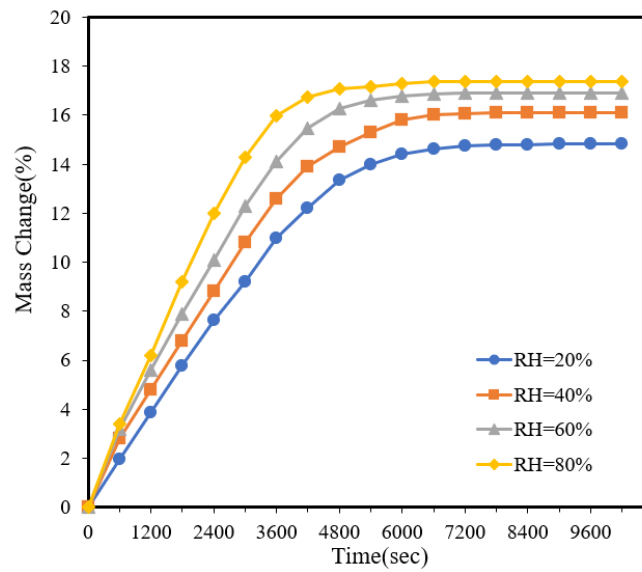
It can be seen that the saturated adsorption capacity of the three adsorbents gradually increased with the increase in humidity when the temperature was constant at $25\text{ }^{\circ}\text{C}$, and the adsorption rate was accelerated and the time required to reach saturation was reduced. For MOF-801, its adsorption characteristics were optimal at $T = 25\text{ }^{\circ}\text{C}$ and $\text{RH} = 80\%$. As shown in Figure 5a, MOF-801 was adsorbed to saturation after 6600 s, and the saturated moisture absorption was 0.279 kg/kg .

As shown in Figure 5b,c, MOF-801/CB was adsorbed to saturation after 5400 s with a saturated moisture uptake of 0.174 kg/kg , while MOF-801/CB-LiCl was adsorbed almost to saturation after 10,200 s with a saturated moisture uptake of 1.029 kg/kg , also in the environment of $T = 25\text{ }^{\circ}\text{C}$ and $\text{RH} = 80\%$. In summary, for all three adsorbents, higher humidity is favorable to increase their adsorption capacity. The saturated adsorption amount of MOF-801/CB-LiCl is higher than that of the other two adsorbents at each humidity.

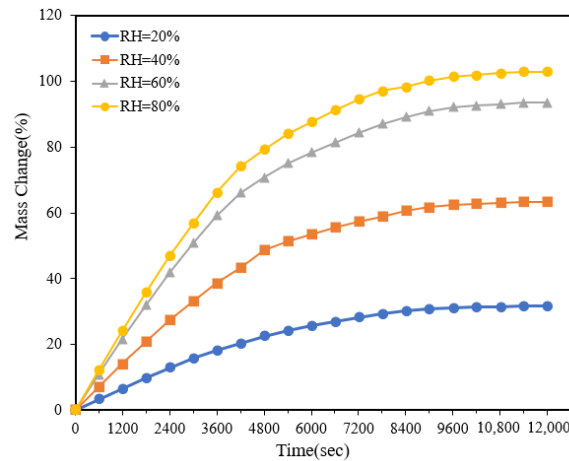


(a)

Figure 5. Cont.



(b)

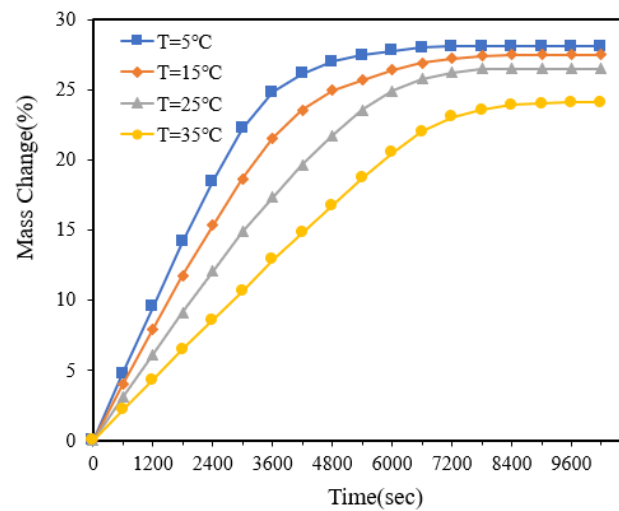


(c)

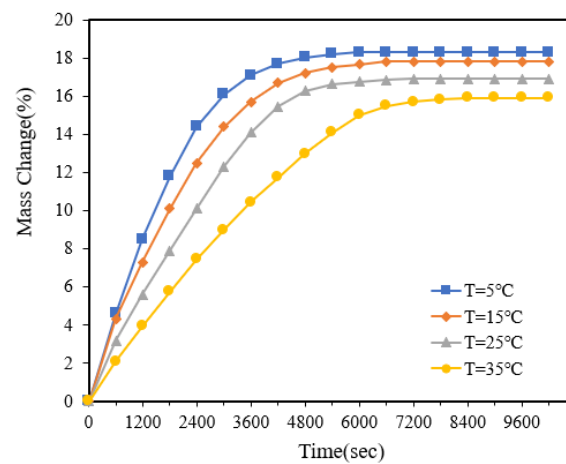
Figure 5. Mass change curves of the three adsorbents when adsorbed at different humidities: (a) MOF-801; (b) MOF-801/CB; (c) MOF-801/CB-LiCl.

The ambient temperature will also have a great influence on the performance of the adsorbent. In order to investigate the adsorption characteristics of the composite adsorbents under different temperatures in detail, adsorption tests were carried out on MOF-801, MOF-801/CB, and MOF-801/CB-LiCl successively. The environmental parameters were set as RH = 60% and T = 5 °C, 15 °C, 25 °C, and 35 °C; the change in the working mass of the adsorbent was recorded until it reached saturation; and the experimental results are shown in Figure 6.

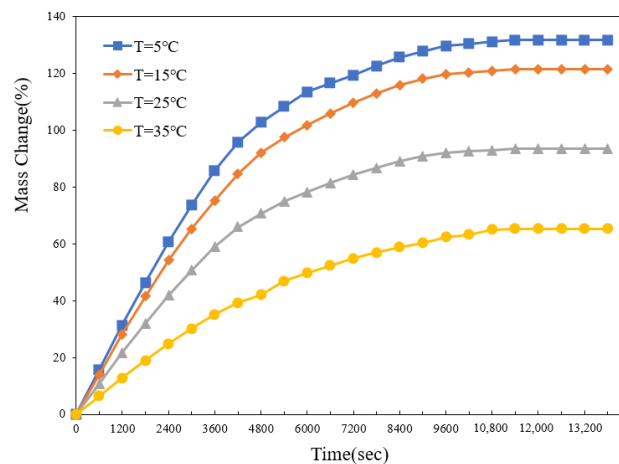
From the experimental results, it can be seen that the saturated adsorption capacity of the three adsorbents gradually increased with decreasing temperature at constant humidity, the adsorption rate was accelerated, and the time required to reach saturation was reduced. For MOF-801, its adsorption characteristics were optimal at RH = 60% and T = 5 °C. As shown in Figure 6a, MOF-801 was adsorbed to saturation after 6000 s, and the saturated moisture absorption was 1.318 kg/kg.



(a)



(b)



(c)

Figure 6. Mass change curves of the three adsorbents for adsorption at different temperatures: (a) MOF-801; (b) MOF-801/CB; (c) MOF-801/CB-LiCl.

As shown in Figure 6b,c, MOF-801/CB was adsorbed to saturation after 4800 s with a saturated moisture adsorption of 0.183 kg/kg, while MOF-801/CB-LiCl was adsorbed to saturation after 11,400 s with a saturated moisture adsorption of 1.029 kg/kg, also in an

environment with RH = 60% and T = 5 °C. In summary, for the three adsorbents, lower temperatures are favorable to improve their adsorption capacity. Meanwhile, the saturated adsorption amount of MOF-801/CB-LiCl was higher than that of the other two adsorbents at all temperatures.

The kinetic constants for water vapor adsorption of the three adsorbents at different temperatures were calculated using the first-order equation of $m_t = m_0(1 - e^{-kt})$, where m_0 is the average moisture adsorption and t is the adsorption time, and the results are shown in Table 1. From the table, it can be seen that the temperature greatly affects the performance of the three adsorbents.

Table 1. Kinetics (k) of water adsorption for the three adsorbents at variable temperatures.

	MOF-801	MOF-801/CB	MOF-801/CB-LiCl
5 °C	k = 0.0311	k = 0.0322	k = 0.0198
15 °C	k = 0.0328	k = 0.0361	k = 0.0226
25 °C	k = 0.0446	k = 0.0461	k = 0.0303
35 °C	k = 0.0506	k = 0.0561	k = 0.0413

4. Experimental Study of Desorption Characteristics of New Composite Adsorbents and Water Intake Analysis

4.1. Desorption Characterization Experiment

The ability to fully desorb determines the water production capacity of the adsorbent. In order to facilitate the desorption performance test of the adsorbent, a water extraction experimental setup as shown in Figure 7 was fabricated according to the size of the Petri dish in the experiment.



Figure 7. Structure of the desorption vessel.

The device consists of two parts, the top and bottom, which are assembled in the center by means of threads for easy disassembly for sample processing. The threaded joints are sealed by gaskets to maintain a tight seal inside the device during the desorption process. The outer wall is made of acrylic material, which ensures the structural strength and facilitates the processing of the structure; has a high thermal resistance and light transmission capacity to ensure that the Petri dish is fully illuminated during the experimental process; and reduces the heat exchange between the outer wall and the surrounding environment to maintain the stability of the temperature of the samples in the Petri dish. The bottom of the device was sealed with acrylate adhesive and an aluminum sheet, and a plastic holder was used to separate the Petri dish from the bottom of the device. When desorption experiments were conducted, the device was placed on a temperature-controlled cold source to facilitate the full heat exchange between the bottom surface and the cold wall, so that the resolved water vapor could condense quickly at the bottom of the device without

affecting the temperature of the adsorbent in the Petri dish, and the condensation effect of the water-cooled wall in the process of desorption is demonstrated in Figure 8.



Figure 8. Condensation on desorption vessel cooling walls.

To prepare for the desorption experiments, the three adsorbents were first adsorbed to saturation at $RH = 60\%$ and $T = 25\text{ }^{\circ}\text{C}$, and then sealed in a desorption vessel. A xenon lamp with a 1.5 AM filter was used to simulate solar illumination in a constant-temperature chamber, and desorption experiments were carried out on the three adsorbents successively, with the radiation intensity set at $E = 1\text{ kW/m}^2$. The proportion of water precipitated during the desorption process was recorded to evaluate the desorption performance of the three adsorbents, and the results of the experiments are shown in Figure 9.

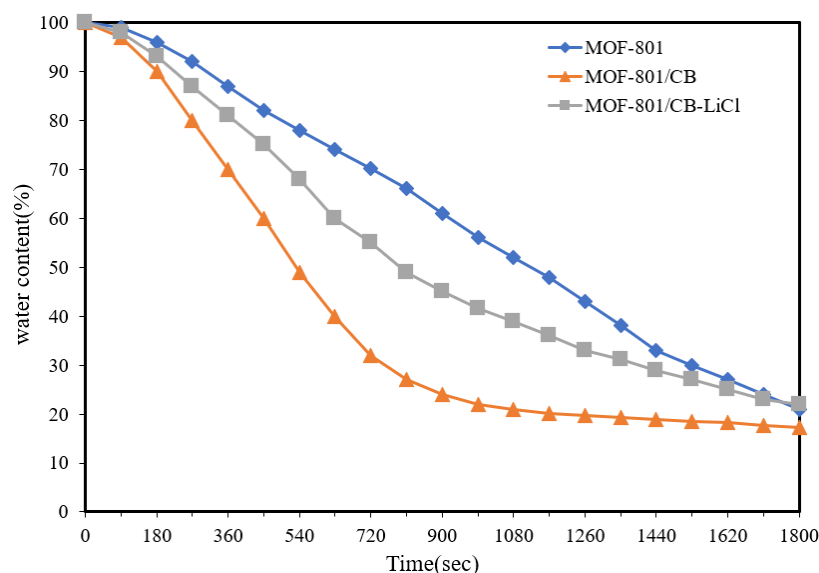


Figure 9. Desorption curves of three adsorbents.

From the experimental results, it can be seen that the desorption rate of both MOF-801/CB and MOF-801/CB-LiCl is superior to that of the MOF-801 adsorbent alone due to the improved photothermal properties of the adsorbent by CB. The adsorption as well as the water yield of MOF-801/CB-LiCl was greatly improved compared to that of MOF-801/CB after the addition of LiCl. Linear fitting shows that the desorption rates of the three adsorbents were 1.78%, 4.45%, and 2.89% per minute for the first 15 min, respectively.

4.2. Evaluation of the Performance of Composite Adsorbents for Water Intake

Based on the above experiments, the performance of the MOF-801/CB-LiCl composite adsorbent in an intermittent air water extraction unit was estimated to evaluate the potential of its application. Estimation of the average daily water withdrawal (W) of the adsorbent is shown in Equation (1):

$$W = \frac{T_0}{T_d + T_a} \times \frac{m_w}{m_a} \quad (1)$$

In the above equation, T_0 is the effective sunshine duration, assumed to be 12 h; $T_a = 125$ min is the length of one adsorption of the device; $T_d = 20$ min is the length of one desorption of the device; m_w is the amount of water extracted from a single cycle of the device; and m_a is the mass of adsorbent in the device.

Combined with the adsorption kinetic parameters, 2.21 kg of fresh water per kg of the MOF-801/CB-LiCl adsorbent can be accessed per day if adsorbed at RH = 60% and T = 15 °C and subsequently desorbed at a solar irradiation intensity of $E = 1$ kW/m².

A comparison of the average daily water production of the intermittent air water extraction device based on the MOF-801/CB-LiCl composite adsorbent and other air water extraction devices is shown in Figure 10, which indicates that the water extraction of this device (In the red box) is higher than most adsorbents, such as silica gel, hygroscopic salt (CaCl₂), and MOF-801, but still lower than hydrogel PAN fiber membranes. However, the preparation and processing of hydrogel PAN fiber membranes based on the modification of the microscopic molecular structure is complicated, the yield needs to be improved, and the stability needs to be further verified. Therefore, the MOF-801/CB-LiCl composite adsorbent, which is only physically mixed, shows better application potential due to the advantages of a higher average daily water yield, simple processing, and good stability.

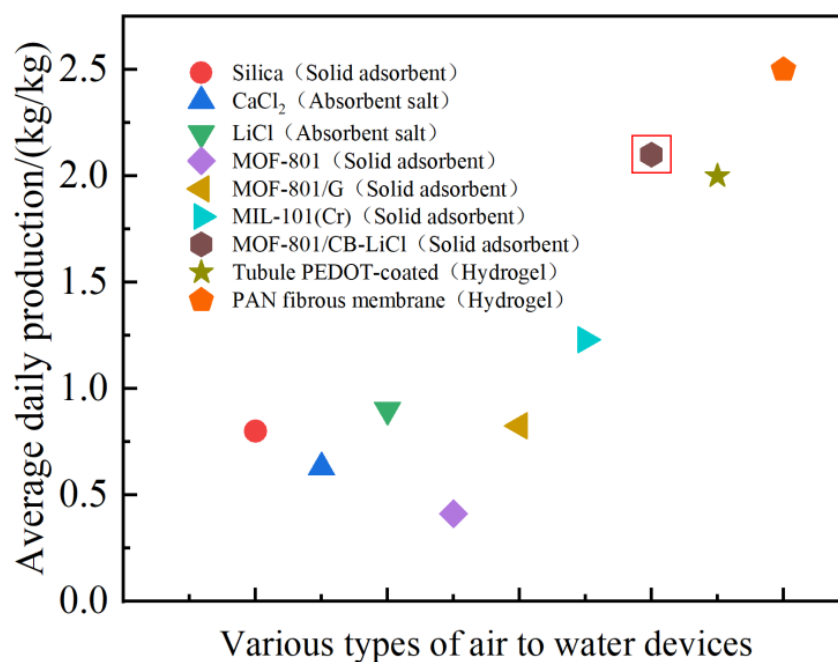


Figure 10. Average daily water production of atmospheric water harvesting driven by solar energy [13,14,18,23–26].

5. Conclusions

In this paper, a new composite adsorbent, MOF-801/CB-LiCl, was prepared by using MOF-801/CB as a substrate and enhancing the adsorption capacity of the adsorbent by the addition of LiCl. Compared to the basic MOF-801 and MOF-801/CB adsorbent, excellent adsorption and desorption characteristics are also ensured while maintaining the

photothermal properties. The following conclusions were drawn from various experimental studies of the new composites:

- (1) The saturated adsorption capacity of MOF-801/CB-LiCl was enhanced by 38.2% and 112.3% compared with that of MOF-801 and MOF-801/CB, respectively, showing that it has high potential for application.
- (2) Higher humidity and lower temperature were favorable to enhance the adsorption capacity of MOF-801/CB-LiCl, and this new adsorbent showed good adsorption characteristics in a wide range of humidity.
- (3) MOF-801/CB-LiCl also has excellent desorption characteristics, which comprehensively enhance the water production capacity of MOF-801. In a continuous solar water removal system, an estimation of 2.21 kg of fresh water per kg of MOF-801/CB-LiCl adsorbent accessible per day was obtained. It has a large advantage over many adsorbents.

Author Contributions: Conceptualization, J.W.; investigation, J.W.; data curation, Y.L. and J.W.; visualization and writing—original draft, Y.L.; writing—review and editing, J.W.; funding acquisition, J.W.; resources, J.D. and T.J.; supervision, J.W. All authors have read and agreed to the published version of the manuscript.

Funding: This research was funded by the Key Program of the National Natural Science Foundation of China, grant number 52130607; the National Natural Science Foundation of China, grant number 52366009; the Double First-Class Key Program of the Gansu Provincial Department of Education, grant number GCJ2022-38; the 2022 Gansu Provincial University Industry Support Plan Project, grant number 2022CYZC-21; and the Key R&D Program of Gansu Province of China, grant number 22YF7GA163. The project is also supported by the Key Laboratory of Power Station Energy Transfer Conversion and Systems of the Ministry of Education.

Institutional Review Board Statement: Not applicable.

Informed Consent Statement: Not applicable.

Data Availability Statement: Data are contained within the article.

Conflicts of Interest: The authors declare no conflicts of interest.

References

1. Tortajada, C.; Biswas, A.K. Water management in post-2020 world. *Int. J. Water Resour. Dev.* **2020**, *36*, 874–878. [[CrossRef](#)]
2. Salehi, M. Global water shortage and potable water safety; Today's concern and tomorrow's crisis. *Environ. Int.* **2022**, *158*, 7. [[CrossRef](#)] [[PubMed](#)]
3. Chen, C.J.; Kuang, Y.D.; Hu, L.B. Challenges and Opportunities for Solar Evaporation. *Joule* **2019**, *3*, 683–718. [[CrossRef](#)]
4. Qi, D.; Zhu, Z.; Li, Y.; Jin, J.; Wu, M. Analysis on the research progress of water intake technology from air. *Appl. Chem. Ind.* **2022**, *51*, 2783–2787.
5. Wang, W.W.; Pan, Q.W.; Wang, R.Z.; Ge, T.S. Modeling and optimization of a honeycombed adsorbent bed for efficient moisture capture. *Appl. Therm. Eng.* **2022**, *200*, 15. [[CrossRef](#)]
6. Abualhamayel, H.I.; Gandhidasan, P. A method of obtaining fresh water from the humid atmosphere. *Desalination* **1997**, *113*, 51–63. [[CrossRef](#)]
7. Ejeian, M.; Entezari, A.; Wang, R.Z. Solar powered atmospheric water harvesting with enhanced LiCl/MgSO₄/ACF composite. *Appl. Therm. Eng.* **2020**, *176*, 11. [[CrossRef](#)]
8. Entezari, A.; Ejeian, M.; Wang, R.Z. Extraordinary air water harvesting performance with three phase sorption. *Mater. Today Energy* **2019**, *13*, 362–373. [[CrossRef](#)]
9. Xu, J.X.; Li, T.X.; Yan, T.S.; Wu, S.; Wu, M.Q.; Chao, J.W.; Huo, X.Y.; Wang, P.F.; Wang, R.Z. Ultrahigh solar-driven atmospheric water production enabled by scalable rapid-cycling water harvester with vertically aligned nanocomposite sorbent. *Energy Environ. Sci.* **2021**, *14*, 5979–5994. [[CrossRef](#)]
10. Lei, C.X.; Guo, Y.H.; Guan, W.X.; Lu, H.Y.; Shi, W.; Yu, G.H. Polyzwitterionic Hydrogels for Efficient Atmospheric Water Harvesting. *Angew. Chem.-Int. Ed.* **2022**, *61*, 5. [[CrossRef](#)]
11. Zhang, W.C.; Xia, Y.; Wen, Z.T.; Han, W.X.; Wang, S.F.; Cao, Y.P.; He, R.X.; Liu, Y.M.; Chen, B.L. Enhanced adsorption-based atmospheric water harvesting using a photothermal cotton rod for freshwater production in cold climates. *RSC Adv.* **2021**, *11*, 35695–35702. [[CrossRef](#)] [[PubMed](#)]
12. William, G.E.; Mohamed, M.H.; Fatouh, M. Desiccant system for water production from humid air using solar energy. *Energy* **2015**, *90*, 1707–1720. [[CrossRef](#)]

13. Srivastava, S.; Yadav, A. Water generation from atmospheric air by using composite desiccant material through fixed focus concentrating solar thermal power. *Sol. Energy* **2018**, *169*, 302–315. [[CrossRef](#)]
14. Wang, F.C.; Zhang, X.; Wang, Q.Q.; Xie, Y.P.; Wang, C.; Zhao, J.H.; Yang, Q.X.; Chen, Z.J. Preparation of MS/MIL-101(Cr) composite material and its properties of atmospheric water collection. *J. Solid State Chem.* **2021**, *304*, 8. [[CrossRef](#)]
15. Nguyen, H.L.; Hanikel, N.; Lyle, S.J.; Zhu, C.H.; Proserpio, D.M.; Yaghi, O.M. A Porous Covalent Organic Framework with Voided Square Grid Topology for Atmospheric Water Harvesting. *J. Am. Chem. Soc.* **2020**, *142*, 2218–2221. [[CrossRef](#)]
16. Fathieh, F.; Kalmutzki, M.J.; Kapustin, E.A.; Waller, P.J.; Yang, J.J.; Yaghi, O.M. Practical water production from desert air. *Sci. Adv.* **2018**, *4*, 9. [[CrossRef](#)]
17. Kim, H.; Rao, S.R.; Kapustin, E.A.; Zhao, L.; Yang, S.; Yaghi, O.M.; Wang, E.N. Adsorption-based atmospheric water harvesting device for arid climates. *Nat. Commun.* **2018**, *9*, 8. [[CrossRef](#)] [[PubMed](#)]
18. Hanikel, N.; Prévot, M.S.; Fathieh, F.; Kapustin, E.A.; Lyu, H.; Wang, H.Z.; Diercks, N.J.; Glover, T.G.; Yaghi, O.M. Rapid Cycling and Exceptional Yield in a Metal-Organic Framework Water Harvester. *ACS Cent. Sci.* **2019**, *5*, 1699–1706. [[CrossRef](#)]
19. Zhao, H.Z.; Huang, T.H.; Liu, T.; Lei, M.; Zhang, M. Synthesis of MgCl₂/vermiculite and its water vapor adsorption-desorption performance. *Int. J. Energy Res.* **2021**, *45*, 21375–21389. [[CrossRef](#)]
20. Xu, J.X.; Li, T.X.; Chao, J.W.; Wu, S.; Yan, T.S.; Li, W.C.; Cao, B.Y.; Wang, R.Z. Efficient Solar-Driven Water Harvesting from Arid Air with Metal-Organic Frameworks Modified by Hygroscopic Salt. *Angew. Chem. -Int. Ed.* **2020**, *59*, 5202–5210. [[CrossRef](#)]
21. Hu, Y.; Fang, Z.; Wan, X.Y.; Ma, X.; Wang, S.L.; Fan, S.K.; Dong, M.Y.; Ye, Z.Z.; Peng, X.S. Carbon nanotubes decorated hollow metal-organic frameworks for efficient solar-driven atmospheric water harvesting. *Chem. Eng. J.* **2022**, *430*, 9. [[CrossRef](#)]
22. Song, Y.; Xu, N.; Liu, G.L.; Qi, H.S.; Zhao, W.; Zhu, B.; Zhou, L.; Zhu, J. High-yield solar-driven atmospheric water harvesting of metal-organic-framework-derived nanoporous carbon with fast-diffusion water channels. *Nat. Nanotechnol.* **2022**, *17*, 857. [[CrossRef](#)] [[PubMed](#)]
23. Sleiti, A.K.; Al-Khawaja, H.; Al-Khawaja, H.; Al-Ali, M. Harvesting water from air using adsorption material—Prototype and experimental results. *Sep. Purif. Technol.* **2021**, *257*, 12. [[CrossRef](#)]
24. Talaat, M.A.; Awad, M.M.; Zeidan, E.B.; Hamed, A.M. Solar-powered portable apparatus for extracting water from air using desiccant solution. *Renew. Energy* **2018**, *119*, 662–674. [[CrossRef](#)]
25. Wang, H.M.; Yang, H.R.; Woon, R.; Lu, Y.; Diao, Y.F.; D'Arcy, J.M. Microtubular PEDOT-Coated Bricks for Atmospheric Water Harvesting. *Acs Appl. Mater. Interfaces* **2021**, *13*, 34671–34678. [[CrossRef](#)]
26. Wu, J.; Zhou, H.; Wang, H.X.; Shao, H.; Yan, G.L.; Lin, T. Novel Water Harvesting Fibrous Membranes with Directional Water Transport Capability. *Adv. Mater. Interfaces* **2019**, *6*, 9. [[CrossRef](#)]

Disclaimer/Publisher's Note: The statements, opinions and data contained in all publications are solely those of the individual author(s) and contributor(s) and not of MDPI and/or the editor(s). MDPI and/or the editor(s) disclaim responsibility for any injury to people or property resulting from any ideas, methods, instructions or products referred to in the content.